

Steady-State Equilibrium Analysis of a Multibody System Driven by Constant Generalized Speeds

Dong Hwan Choi, Jung Hun Park, Hong Hee Yoo*

School of Mechanical Engineering, Hanyang University, Seoul 133-791, Korea

A formulation which seeks steady-state equilibrium positions of constrained multibody systems driven by constant generalized speeds is presented in this paper. Since the relative coordinates are employed, constraint equations at cut joints are incorporated into the formulation. To obtain the steady-state equilibrium position of a multibody system, nonlinear equations are derived and solved iteratively. The nonlinear equations consist of the force equilibrium equations and the kinematic constraint equations. To verify the effectiveness of the proposed formulation, two numerical examples are solved and the results are compared with those of a commercial program.

Key Words : Steady-State Equilibrium, Multibody System, Relative Coordinate, Nonlinear Equation

1. Introduction

A formulation which employs relative coordinates and seeks steady-state equilibrium positions of multibody systems driven by constant generalized speeds is presented in this paper. The proposed method has an advantage of obtaining the equilibrium positions directly by using iterative method. Therefore there is no need to integrate system equation of motion. In case of using available commercial programs, however, the steady-state equilibrium positions can be obtained by performing dynamic analysis with a proper artificial damping. Various kinds of the conventional static equilibrium analysis methods (Nikravesh, 1988; Haug, 1988; Nikravesh and Srinivasan, 1985; Kim et al., 1999), which determine a correct set of coordinates prior to a dynamic analysis, have been proposed. But with these conventional methods, steady-state equilibrium positions of multibody system driven by

constant generalized speeds cannot be found.

An analytical method of finding steady-state equilibrium positions of multibody system with constant generalized speeds is presented in Kane and Levinson (1985). With this method, if the kinetic energy function does not involve time explicitly, the steady-state equilibrium positions of the system can be obtained by setting the partial derivatives of the system Lagrangian with respect to system generalized coordinates at zero. However, rather simple systems can be solved with this method and a method of determining proper system generalized coordinates efficiently has not been suggested. In general, if Cartesian coordinates are employed for the system driven by constant generalized speeds, the steady-state equilibrium positions cannot be found since the positions are varied with time. In this paper, therefore, the relative coordinates (Kim and Vanderploeg, 1986; Bae and Haug, 1987a) are employed as system generalized coordinates. For the open-loop system, equations of motion are derived without constraint equations while for the closed-loop system, the constraint equations of cut joints (Bae and Haug, 1987b) are supplemented to the equations of motion. In order to find steady-state equilibrium positions of multi-

* Corresponding Author,

E-mail : hhyoo@hanyang.ac.kr

TEL : +82-2-2290-0446; FAX : +82-2-2293-5070

School of Mechanical Engineering, Hanyong University, Seoul 133-791, Korea. (Manuscript Received August 30, 2001; Revised July 5, 2002)

body systems driven by constant generalized speeds, system generalized coordinates are partitioned into the coordinates of constant generalized speeds and the rest of the system generalized coordinates. The proposed method can be applied to both open and closed loop systems. Force equilibrium equations (for open and closed loop systems) and kinematic constraint equations (for closed loop systems) constitutes nonlinear equations that need to be solved iteratively to obtain the steady-state equilibrium positions. Therefore the proposed method has the advantage of obtaining the equilibrium positions directly since it doesn't need to solve differential equations.

2. Equations of Motion

A general rigid body can be represented in three-dimensional space by six coordinates. Three of the coordinates define the orientation of the body and the other three coordinates define the translational position. All six coordinates are defined with respect to an inertial reference frame. The orientation coordinates are normally obtained using three successive rotational angles about an orthogonal axis.

Consider a body i in a three dimensional space shown in Fig. 1. Let $X-Y-Z$ be the global coordinate system with origin O and $x_i-y_i-z_i$ be the body fixed coordinate system with O_i . The vector bold r_i is a vector that defines the global

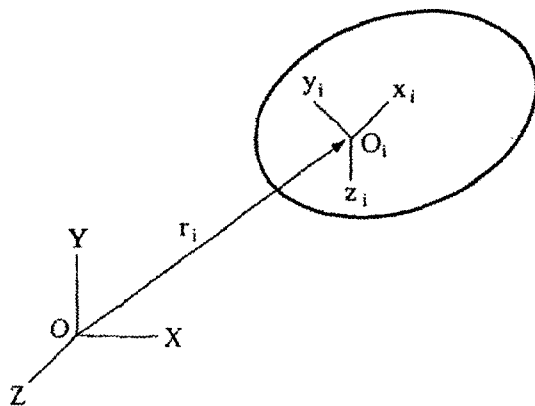


Fig. 1 A moving body in space

position of the origin O_i . In this paper, a generalized Cartesian coordinates for body i in a multibody system are defined as

$$x_i = [r_i^T \ \theta_i^T]^T \tag{1}$$

where the set θ_i is a set of generalized rotational coordinates that define the orientation of the body i .

In general, the augmented Lagrange equations of motion for a constrained multibody system in terms of Cartesian coordinates are derived as

$$M\ddot{x} + \Phi_x^T \lambda = Q \tag{2}$$

where M is a system mass matrix, Q is a generalized force vector, Φ_x is the Jacobian matrix of constraint equations with respect to Cartesian coordinates, and λ is a vector of Lagrange multipliers. The constraint equations are partitioned as

$$\Phi = [\Phi^{cT} \ \Phi^{rT}]^T \tag{3}$$

In the above equation, Φ^c represent kinematic constraints from cut joints in closed loop system and Φ^r represent the rest constraints. Figure 2 shows Φ^c and Φ^r for a simple closed loop system. In this paper, the system generalized coordinate q_i can be defined as the relative coordinates determined by the type of joint between body i and its reference body. Generally, the Cartesian

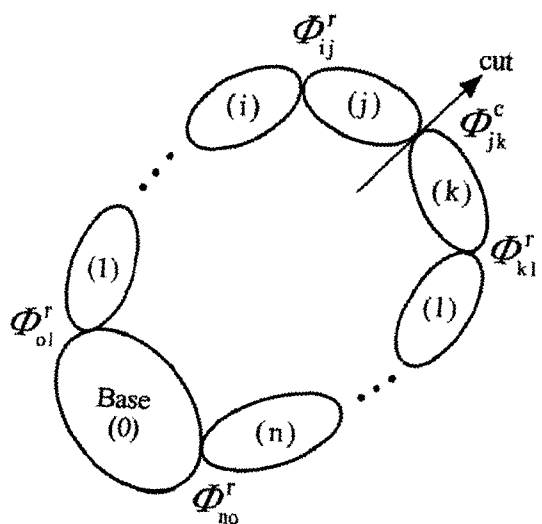


Fig. 2 A schematic representation of a closed loop system

velocity vector of a multibody system can be represented in terms of relative velocity vector by velocity transformation (Kim and Vanderploeg, 1986; Bae and Haug, 1987a) as

$$\dot{\mathbf{x}} = \mathbf{B}\dot{\mathbf{q}} \quad (4)$$

where \mathbf{B} is the velocity transformation matrix, and the system Cartesian velocity vector $\dot{\mathbf{x}}$ and the system generalized velocity vector $\dot{\mathbf{q}}$ are defined as

$$\dot{\mathbf{x}} = [\dot{\mathbf{x}}_1^T \ \dot{\mathbf{x}}_2^T \ \cdots \ \dot{\mathbf{x}}_n^T]^T \quad (5)$$

$$\dot{\mathbf{q}} = [\dot{q}_1 \ \dot{q}_2 \ \cdots \ \dot{q}_p]^T \quad (6)$$

In the above equations, n represents the number of bodies and p represents the number of relative coordinates.

In order to derive the equations of motion for the system with constant generalized speeds, the system generalized coordinates \mathbf{q} are partitioned into \mathbf{q}_D (the coordinates which involve with constant generalized speeds) and \mathbf{q}_R (the rest generalized coordinates).

$$\mathbf{q} = [\mathbf{q}_D^T \ \mathbf{q}_R^T]^T \quad (7)$$

Figure 3 shows the generalized coordinates \mathbf{q}_D and \mathbf{q}_R for a simple system. Therefore, the system Cartesian velocity vector $\dot{\mathbf{x}}$ can be represented in terms of $\dot{\mathbf{q}}_D$ and $\dot{\mathbf{q}}_R$ as

$$\dot{\mathbf{x}} = \mathbf{B}_D\dot{\mathbf{q}}_D + \mathbf{B}_R\dot{\mathbf{q}}_R \quad (8)$$

where $\dot{\mathbf{q}}_D$ represents constant generalized speeds and $\dot{\mathbf{q}}_R$ represents the time derivatives of \mathbf{q}_R . And the velocity transformation matrix and \mathbf{B}_D and \mathbf{B}_R are sub-matrices associated with the coordinates \mathbf{q}_D and \mathbf{q}_R . Therefore, \mathbf{B} is composed \mathbf{B}_D and \mathbf{B}_R as

$$\mathbf{B} = [\mathbf{B}_D \ \mathbf{B}_R] \quad (9)$$

Similarly the system Cartesian acceleration vector is obtained by taking the time derivative of Eq. (8)

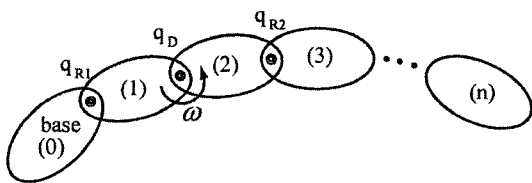


Fig. 3 Generalized coordinates \mathbf{q}_D and \mathbf{q}_R

$$\dot{\mathbf{x}} = \mathbf{B}_D\dot{\mathbf{q}}_D + \mathbf{B}_R\dot{\mathbf{q}}_R + \dot{\mathbf{B}}_D\dot{\mathbf{q}}_D + \dot{\mathbf{B}}_R\dot{\mathbf{q}}_R \quad (10)$$

Substituting Eqs. (3) and (10) into Eq. (2) and premultiplying Eq. (2) by \mathbf{B}_R^T , one obtains

$$\mathbf{B}_R^T [\mathbf{M} (\mathbf{B}_D\dot{\mathbf{q}}_D + \mathbf{B}_R\dot{\mathbf{q}}_R + \dot{\mathbf{B}}_D\dot{\mathbf{q}}_D + \dot{\mathbf{B}}_R\dot{\mathbf{q}}_R) + \Phi_x^{cT}\lambda^c + \Phi_x^{cT}\lambda^r] = \mathbf{B}_R^T \mathbf{Q} \quad (11)$$

Since $\dot{\mathbf{q}}_D$ is constant vector, $\dot{\mathbf{q}}_D$ is identically zero vector. The constraint Jacobian matrix with respect to the generalized coordinates \mathbf{q}_R , Φ_{q_R} can be obtained using the chain rule of differentiation and the dot cancellation law (Rosenberg, 1977) as

$$\Phi_{q_R} = \frac{\partial \Phi}{\partial \mathbf{x}} \frac{\partial \mathbf{x}}{\partial \mathbf{q}_R} = \Phi_x \frac{\partial \dot{\mathbf{x}}}{\partial \dot{\mathbf{q}}_R} = \Phi_x \mathbf{B}_R \quad (12)$$

Since the velocity transformation matrix \mathbf{B}_R is the null space of the constraint Jacobian matrix Φ_x , the following equation is obtained.

$$\mathbf{B}_R^T \Phi_x^T = 0 \quad (13)$$

Using the Eq. (13), Eq. (11) can be rewritten as

$$\mathbf{M}^* \dot{\mathbf{q}}_R + \Phi_{q_R}^{cT} \lambda^c = \mathbf{Q}^* \quad (14)$$

where

$$\mathbf{M}^* = \mathbf{B}_R^T \mathbf{M} \mathbf{B}_R \quad (15)$$

$$\mathbf{Q}^* = \mathbf{B}_R^T \mathbf{Q} - \mathbf{B}_R^T (\mathbf{M} \dot{\mathbf{B}}_D \dot{\mathbf{q}}_D + \mathbf{M} \dot{\mathbf{B}}_R \dot{\mathbf{q}}_R) \quad (16)$$

Since $\dot{\mathbf{q}}_D$ is identically zero vector, the constraint acceleration equations, the second time derivatives of the constraint equations ($\Phi^c = 0$), can be written as

$$\Phi_{q_R}^c \dot{\mathbf{q}}_R = \boldsymbol{\gamma}^c \quad (17)$$

where the vector $\boldsymbol{\gamma}^c$ which involves second partial derivative terms is defined as

$$\boldsymbol{\gamma}^c = - (\Phi_{q_R}^c \dot{\mathbf{q}}_R)_{q_R} \dot{\mathbf{q}}_R - 2 \Phi_{q_R t}^c \dot{\mathbf{q}}_R - \Phi_{tt}^c \quad (18)$$

Combining Eq. (14) and Eq. (17), the system equations of motion can be written in a matrix form as follows:

$$\begin{bmatrix} \mathbf{M}^* & \Phi_{q_R}^{cT} \\ \Phi_{q_R}^c & 0 \end{bmatrix} \begin{bmatrix} \dot{\mathbf{q}}_R \\ \lambda^c \end{bmatrix} = \begin{bmatrix} \mathbf{Q}^* \\ \boldsymbol{\gamma}^c \end{bmatrix} \quad (19)$$

Therefore, the dynamic analysis of a constrained multibody system driven by constant generalized speeds can be performed by using Eq. (19).

3. Equilibrium Analysis

At steady-state, bold \dot{q}_R and its time derivatives \ddot{q}_R become zero. Therefore Eq. (14) becomes as

$$B_R^T [M\dot{B}_D\dot{q}_D - Q] + \Phi_{q_R}^{cT} \lambda^c = 0 \quad (20)$$

To find the steady-state equilibrium positions, the Eq. (20) and the constraint equations ($\Phi^c=0$) are to be solved simultaneously. Therefore the algorithm which seeks the steady-state equilibrium positions leads to nonlinear equations which consist of the force equilibrium equations and the kinematic constraint equations. To solve the nonlinear equations, the iterative Newton-Raphson procedure is employed as follows :

$$f_z \Delta z^i = -f \quad (21)$$

$$z^{i+1} = z^i + \Delta z^i \quad (22)$$

where

$$f = \left[\begin{matrix} B_R^T [M\dot{B}_D\dot{q}_D - Q] + \Phi_{q_R}^{cT} \lambda^c \\ \Phi^c \end{matrix} \right] \quad (23)$$

$$z = [q_R^T \lambda^{cT}]^T \quad (24)$$

In the above equation, the Jacobian matrix f_z represents $\partial f / \partial z$.

Application of the present algorithm is as same as that given for the static equilibrium analysis problem except that not only initial conditions for positions but also those for generalized speeds should be provided to solve the algebraic equations. Of course, the formulation for the steady-state equilibrium analysis is different from that of the static equilibrium analysis. However, those two formulations are all algebraic equations which can be solved by the Newton-Raphson's method.

4. Numerical Examples

4.1 2 DOF swing pendulum driven by a constant angular velocity

Two DOF (degree of freedom) swing pendulum system driven by a constant angular velocity ($\omega=20$ rad/s) is shown in Fig. 4. This is a typical open loop system that undergoes planar motion. Ground and body 1, and body 1 and body 2

Table 1 Inertia properties of the swing pendulum

Body	Mass [kg]	Moment of inertia $I_{z'z'}$ [kg/m ²]
Body 1	1.0	0.1
Body 2	0.0	0.0
Body 3	1.0	0.0

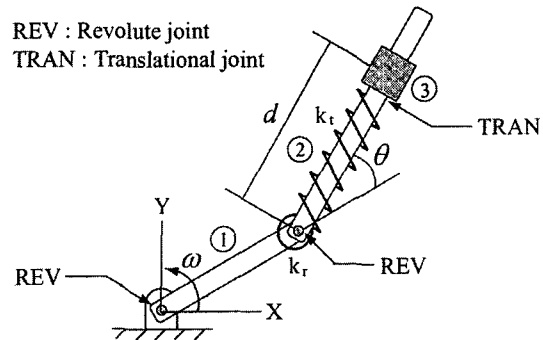


Fig. 4 2-DOF swing pendulum driven by constant angular velocity

are connected by revolute joints respectively. Body 2 and body 3 are connected by translational joint. And body 1 and body 2 are connected by the rotational spring. The stiffness and the undeformed angle of the spring are $k_r=300$ Nm/rad and 1.0472 rad, respectively. Body 2 and body 3 are connected by the translational spring. The stiffness and the undeformed length of the spring are $k_t=50000$ N/m and 1.0 m, respectively. At initial state, the relative angle θ between body 1 and body 2 is 0 rad and the relative distance d is 1.0 m. The length of body 1 is 1.0 m. The mass and inertia properties of this system are given in Table 1.

From the equilibrium analysis, Fig. 5 shows the relative angle θ between body 1 and body 2. At steady-state, Fig. 5 shows that the equilibrium position obtained by the proposed method (marked by a wedge) and the result obtained by ADAMS[10] are almost identical. In this figure, c_r and c_t are rotational and translational damping coefficient, respectively. Table 2 shows the ADAMS simulation data. Figure 6 represents relative distance d between body 2 and body 3. At steady-state, the equilibrium position obtained by the proposed method and the result obtained

by ADAMS(with a proper damping) are almost identical. However, in case of using the com-

Table 2 ADAMS simulation data

ADAMS Simulation Data	Setting values
Simulation Type	Dynamics
Integrator	Gear (GSTIFF)
Step	5000
Step Size	0.001
Corrector Convergence tolerance	1.0E-8
Integrator Order	Max Possible
Upper bound for the maximum number of iteration	20
Jacobian Evaluation	Every iteration
Linear Solver	Harwell

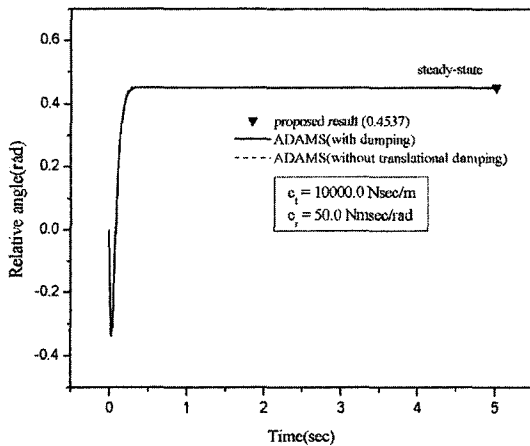


Fig. 5 Relative angle between body 1 and body 2

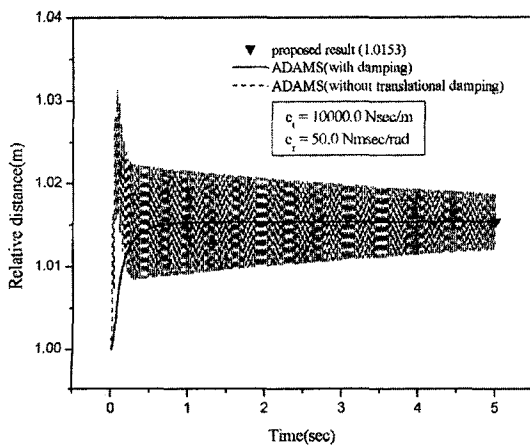


Fig. 6 Relative distance between body 2 and body 3

mercial program, if there is no damping, the steady-state equilibrium positions are not found by the conventional method. In this paper, however, there is no need to assign a proper damping data in order to find steady-state equilibrium positions. Therefore these analysis results show that the proposed algorithm is accurate and efficient compared to the conventional method which performs dynamic analysis.

4.2 Governor mechanism driven by a constant angular velocity

A governor mechanism is shown in Fig. 7. This system is 1 DOF closed loop system. The spindle is driven by a constant angular velocity of 11.0174 rad/s. In this figure, the bodies 1, 2, 3, and 4 represent spindle, ball, ball and collar, respectively. Ground and body 1, body 1 and body 2, and body 1 and body 3 are connected by revolute joints. Body 1 and body 4 are connected by translational joint. Body 2 and body 4, and body 3 and body 4 are connected by distance joints with distance of 0.10922 m. Body 1 and body 4 are connected by the translational spring. The stiffness and the undeformed length of the spring are $k_t=1000$ N/m and 0.15 m, respectively. At initial state, the relative distance between

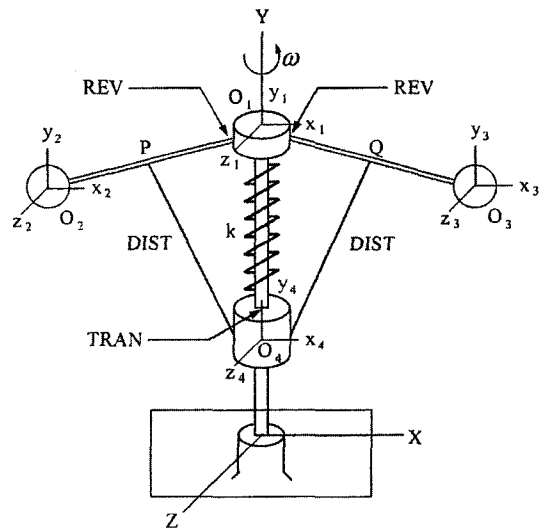


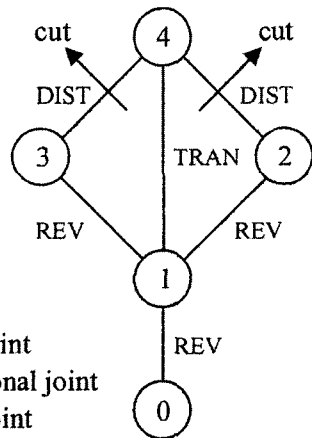
Fig. 7 Governor mechanism driven by constant angular velocity

Table 3 Inertia properties of the governor mechanism

Body	Mass [kg]	Moment of inertia [kg·m ²]		
		I _{x'x'}	I _{y'y'}	I _{z'z'}
Spindle	200.0	25.0	50.0	25.0
Ball 1	1.0	0.1	0.1	0.1
Ball 2	1.0	0.1	0.1	0.1
Collar	1.0	0.15	0.125	0.15

Table 4 Initial values of the governor mechanism

Point	Initial Position [m]
O ₁	[0.0, 0.2, 0.0]
O ₂	[-0.16, 0.2, 0.0]
O ₃	[0.16, 0.2, 0.0]
O ₄	[0.0, 0.1256, 0.0]
P	[-0.08, 0.2, 0.0]
Q	[0.08, 0.2, 0.0]



REV : Revolute joint
 TRAN : Translational joint
 DIST : Distance joint

Fig. 8 Tree structure of the governor mechanism

spindle and collar is 0.0744 m and the relative angles between spindle and balls are 0 rad, and the orientations of all the bodies are parallel to the orientation of the inertial reference frame. Table 3 shows the mass and inertia properties of the system. Table 4 shows initial positions of the governor mechanism. Figure 8 shows the topology of the system using graph theory. In this figure, the number inside a circle represents body number and the line represents joint type. Since the governor mechanism is the closed loop system, the distance joints between collar and balls

Table 5 ADAMS simulation data

ADAMS Simulation Data	Setting values
Simulation Type	Dynamics
Integrator	Gear(GSTIFF)
Step	10000
Step Size	0. 01
Corrector Convergence tolerance	1.0E-8
Integrator Order	Max Possible
Upper bound for the maximum number of iteration	20
Jacobian Evaluation	Every iteration
Linear Solver	Harwell

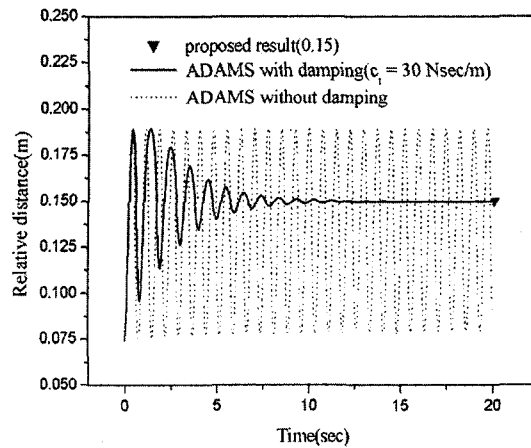


Fig. 9 Relative distance between spindle and collar

become cut joints as shown in Fig. 8.

From the equilibrium analysis, Fig. 9 shows the relative distance between spindle and collar. Table 5 shows the ADAMS simulation data. At steady-state, Fig. 9 shows that the equilibrium position obtained by the proposed algorithm and the result obtained by ADAMS (with a proper damping) are almost identical. Therefore, these analysis results show that the proposed algorithm is accurate and efficient for a closed loop system as well as for an open loop system.

5. Conclusions

A formulation which seeks the steady-state equilibrium positions of constrained multibody systems driven by constant generalized speeds is

presented. The method proposed in this paper, compared to the conventional method of using dynamic analysis with a proper damping, has the advantages of obtaining the equilibrium positions directly by solving nonlinear equations. The accuracy and the effectiveness of the proposed method are confirmed through two numerical examples.

Acknowledgment

This research was supported by Innovative Design Optimization Technology Engineering Research Center through research fund, for which authors are grateful.

References

- ADAMS (Version 11.0) User's Guide*, 2001, Mechanical Dynamics, Inc.
- Bae, D. S. and Haug, E. J., 1987, "A Recursive Formulation for Constrained Mechanical System Dynamics: Part I. Open Loop Systems," *Mech. Struct. & Mach.*, Vol. 15, No. 3, pp. 359~382.
- Bae, D. S. and Haug, E. J., 1987, "A Recursive Formulation for Constrained Mechanical System Dynamics: Part II. Closed Loop Systems," *Mech. Struct. & Mach.*, Vol. 15, No. 4, pp. 481~506.
- Haug, E. J., 1989, *Computer-Aided Kinematics and Dynamics of Mechanical Systems*, Volume I: Basic Method, ALLYN AND BACON.
- Kane, T. R. and Levinson, D. A., 1985, *Dynamics: Theory and Applications*, McGraw-Hill.
- Kim, J. I., Park, J. H., Yoo, H. H. and Bae, D. S., 1999, "Static Equilibrium and Linear Vibration Analysis of Constrained Multibody Systems," *Transactions of KSME (A)*, Vol. 23, No. 5, pp. 871~880.
- Kim, S. S. and Vanderploeg, M. J., 1986, "A General and Efficient Method for Dynamic Analysis of Mechanical Systems Using Velocity Transformations," *ASME Journal of Mechanisms, Transmissions and Automation in Design*, Vol. 108, pp. 176~182.
- Nikravesh, P. E., 1988, *Computer-Aided Analysis of Mechanical Systems*, Prentice-Hall International Editions.
- Nikravesh, P. E. and Srinivasan, M., 1985, "Generalized Coordinate Partitioning in Static Equilibrium Analysis of Large-Scale Mechanical Systems," *International Journal for Numerical Methods in Engineering*, Vol. 21, pp. 451~464.
- Rosenberg, R. M., 1977, *Analytical Dynamics of Discrete Systems*, Plenum Press.